CLIMATOLOGY OF THE SNAKE RIVER PLAIN CONVERGENCE ZONE

Thomas A. Andretta

NOAA/National Weather Service Forecast Office
Pocatello-Idaho Falls, Idaho

Abstract

The climatology of the Snake River Plain Convergence Zone (SPCZ) is examined using observational and high-resolution model data sets. This convergence zone is confined to the planetary boundary later and is formed by the merger of low-level north to northeast winds in the Upper Snake River Plain with low-level southwest to west winds in the eastern Magic Valley and Lower Snake River Plain of eastern Idaho. The SPCZ is initiated by the passage of a synoptic-scale cold front, which aligns the flow to a northwest direction through the Big Lost, Little Lost, and Birch Creek Valleys in central Idaho. This manuscript examines a six-year climatology of this mesoscale feature based on mean antecedent synoptic characteristics obtained from 27 SPCZ cases covering the period November 1995 to November 2001. The prevailing wind patterns for different stations in the path of the mesoscale boundary are analyzed. The evolution and structure of the SPCZ is documented for Type A and Type B patterns based on wind and radar reflectivity signatures. Finally, a multiple variable linear regression formula was derived to calculate (from Meso Eta model parameters) the amplitude (Z coefficient) of the convergence, probability of occurrence, and estimates of the resulting precipitation and snowfall for Idaho Falls and Pocatello. The scheme was applied to an SPCZ episode on 4 January 2002. The Meso Eta and MM5 model fields provided a realistic simulation of the event with these results: Z coefficient of approximately 1.0; probability of occurrence of 35 to 40%; and model precipitation and snowfall amounts verifying close to the observations.

1. Introduction

Planetary boundary layer convergence zones of winds, clouds and precipitation induced by regional topography are frequent phenomena in the diverse geography of the United States. One example is the Puget Sound Convergence Zone (PSCZ) formed by topographic channeling of onshore flow (Mass 1981; Mass and Dempsey 1985; Chien and Mass 1997) around the Olympic Mountains through the Strait of Juan de Fuca and the Chehalis Gap. A second noteworthy example is the Longmont Anticyclone of northeast Colorado (Wesley et al. 1995) as demonstrated during the Winter Icing and Storms Project (WISP) (Rasmussen et al. 1992).

The Snake River Plain Convergence Zone (SPCZ) was observed and forecast by operational meteorologists at the NOAA/National Weather Service (NWS) Weather Forecast Office (WFO) in Boise, Idaho using limited data sets and without the benefit of radar coverage over eastern Idaho. Concomitant with the NWS Weather Surveillance Radar – 1988 Doppler (WSR-88D) deployment at Springfield, Idaho in July 1995 and the spin-up of the NWS WFO in Pocatello-Idaho Falls, numerous boundary layer convergence episodes have been examined by operational forecasters using mesonet wind and radar data observations. Andretta and Hazen (1998) documented the genesis and decay of an SPCZ event, which occurred on 26 November 1995. They based their study on the Air Resources Laboratory, Field Research Division's (ARL/FRD) automated mesonet 15-m wind towers and the NWS WSR-88D base velocity and composite reflectivity fields. This SPCZ formed over the upper part of the Snake River Plain (SRP) in the moist and unstable airmass behind a surface Pacific cold front. The boundary propagated south at about 10 knots over the SRP, producing moderate to heavy snow over parts of the SRP. The SPCZ analysis was subdivided into formation, persistence, and dissipation stages based on a combination of radar and mesonet wind signatures.

This study explores the antecedent synoptic conditions favorable to SPCZ formation based on 27 case studies covering the period from November 1995 to November 2001. Using model and observed data, wind direction and speed climatologies are obtained for stations affected by the SPCZ. Radar climatology using base radial velocity (0.5 degrees) and composite reflectivity data are explored for distinct synoptic flow SPCZ patterns. An intensity scale (Z coefficient) is also presented for the SPCZ to measure the ratio of observed low-level wind speeds over the SRP. Using this scale, a multiple regression equation is derived to forecast the amplitude of the SPCZ, probability of occurrence, and precipitation amounts for Idaho Falls (in the Upper Snake River Plain) and Pocatello (in the Lower Snake River Plain) using the 22-km Meso Eta model. These output variables are listed in a guidance table to aid operational forecasters in the prediction of this mesoscale phenomenon. The forecasting scheme is applied to the SPCZ event, which occurred on 4 January 2002.

a. Region of study

Figures 1a and 1b illustrate the geographical regions of study with Idaho (hatched region) and the shaded inset region denoting the local area of study. Figures 1c and 1d display the ARL/FRD and NWS METAR stations used in the mesonet and WSR-88D analyses, respectively. The

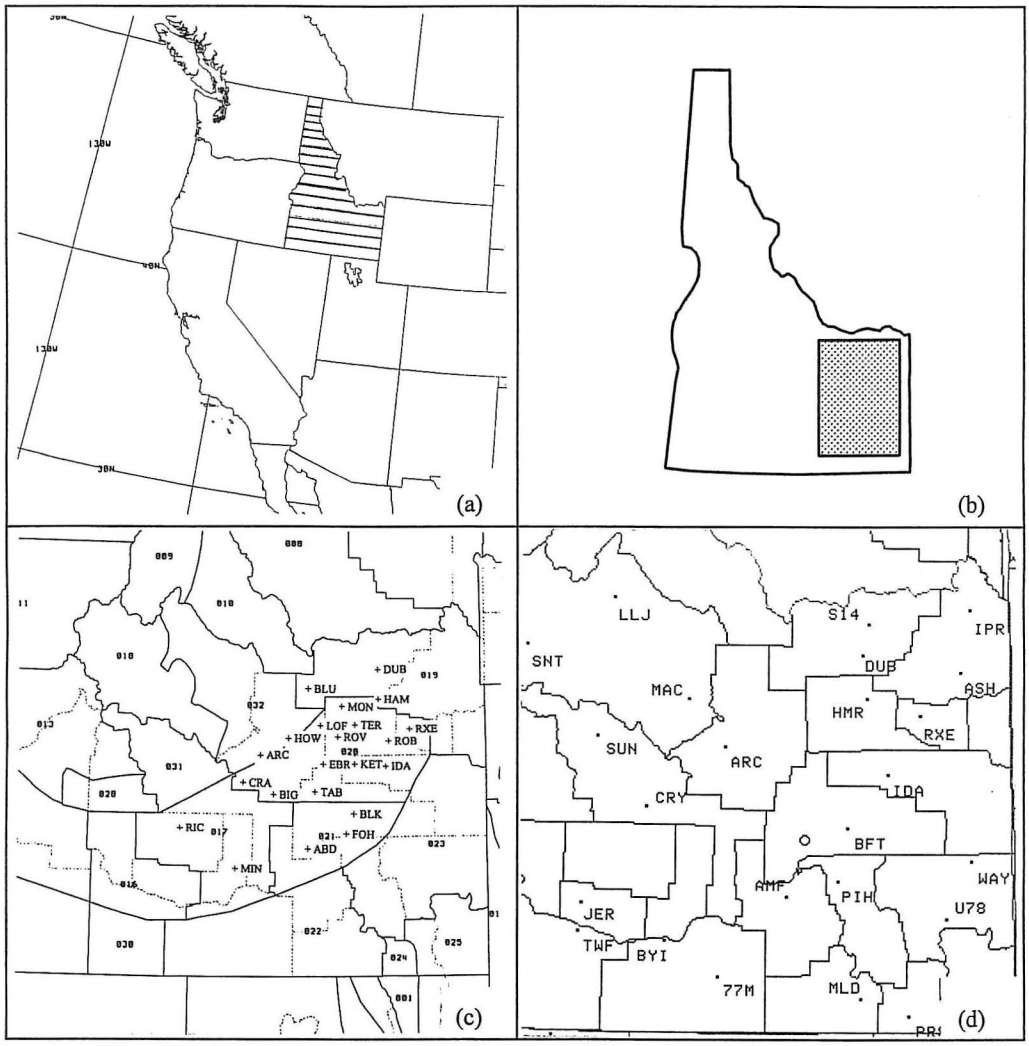

Fig. 1. Reference locations: (a) map of Northwest United States with state of Idaho (hatched region), (b) map of Idaho with study area of eastern Idaho (shaded region), (c) ARL/FRD stations (3-letter identifiers), counties (dashed lines), zone boundaries (solid lines), and 3-digit zone numbers, and (d) NWS METAR stations, city locations, counties (solid lines) and Springfield, Idaho WSR-88D tower (open circle).

numbered zone regions, which define areas of significant climatological similarity are indicated in Fig. 1c. Tables 1a and 1b summarize the key zone numbers, station identifiers, and station names for Idaho referenced in the manuscript.

b. Data sources

The ARL/FRD operates and maintains the joint NOAA and Department of Energy (DOE) mesonet comprised of 31, instrumented, 15-m towers located throughout the SRP. The wind data from the NOAA/DOE mesonet are used to measure the flow patterns during the various phases of the SPCZ. The NWS (KSFX) WSR-88D is located near Springfield, Idaho (open circle; Fig. 1d) at an approximate elevation of 1.4 km MSL. The lowest tilt angle (0.5 degrees) of the base radial velocity and composite reflectivity data from the KSFX WSR-88D are used to analyze the structure of SPCZs during the development, persistence, and dissipation stages. For clarification, the composite reflectivity is defined as the highest base reflectivity value measured in a vertical column above the indicated location for all elevation angles during the volume scan.

2. The Snake River Plain Convergence Zone (SPCZ)

a. Topography of eastern Idaho

The 22-km Meso Eta model (Staudenmaier 1996; Manikin et al. 2000) and 12-km MM5 model (Grell et al. 1995; Dudhia et al. 1999) were selected to simulate the evolution and structure of the SPCZ based on their fine horizontal and vertical resolutions. The MM5 is run by the University of Utah and output is distributed from the NWS office in Salt Lake City, Utah to other NWS offices in the western United States. Further information regarding the MM5 model can be found at Web site address: http://www.met.utah.edu/jimsteen/mm5/description.html.

Figures 2a and 2b depict the topography for eastern Idaho in both of the models used. The terrain of eastern Idaho is dominated by the SRP, which is roughly 100 km wide and is oriented from southwest to northeast with a gradual increase in elevation from approximately 1.3 km near American Falls (AMF) to 1.5 km near Rexburg (RXE) (all heights MSL). (Please refer to Figs. 1c, 1d and 2c for location names, identifiers and zones.) The region of the SRP north of Blackfoot (BFT) to Arco (ARC) is defined as the Upper Snake River Plain (USRP) or Zone 20; the region south to AMF and Pocatello (PIH) is defined as the Lower Snake River Plain (LSRP) or Zone 21. In addition, the (eastern) Magic Valley (Zone 17) (average elevation ~ 0.8 km) lies west of and rises into the Lower Snake River Plain (average elevation ~ 1.1 km). All these regions are well depicted in the Meso Eta and MM5 model terrains (Figs. 2a and 2b), with a 1.0 km height contour over the eastern Magic Valley and a 1.5 km height contour encircling the USRP and LSRP.

Other important geographic features include: the Upper Snake (Zone 19) and Caribou Highlands (Zone 23) (average elevation ~ 2.0 km) (Fig. 1c), which define the east and southeast boundary of the USRP and LSRP

TABLE 1a: Zone Numbers, Station Identifiers, and Station Names in Idaho

Zone Number	Station Identifier	Station Name
17	BYI	Burley
17	MIN	Minidoka
17	RIC	Richfield
19	ASH	Ashton
19	BLU	Blue Dome
19	DUB	Dubois
19	IPR	Island Park
19	S14	Spencer
20	BIG	Big Southern Butte
20	CRA	Craters of Moon
20	EBR	EBR2
20	HAM, HMR	Hamer
20	IDA	Idaho Falls
20	KET	Kettle Butte
20	LOF	Loft
20	MON	Monteview
20	ROB	Roberts
20	ROV	Rover
20	RXE	Rexburg
20	TAB	Taber
20	TER	Terreton

TABLE 1b: Zone Numbers, Station Identifiers, and Station Names in Idaho

Zone Number	Station Identifier	Station Name
21	ABD	Aberdeen
21	AMF	American Falls
21	BFT, BLK	Blackfoot
21	FOH	Fort Hall
21	PIH	Pocatello
22	77M	Malta
22	MLD	Malad
23	U78	Soda Springs
23	WAY	Wayan
31	CRY	Carey
31	SUN	Sun Valley
32	ARC	Arco
32	HOW	Howe
32	LLJ	Challis
32	MAC	Mackay

respectively and the Central Mountains (average elevation ~ 2.8 km) that define the west and northwest boundary of the USRP and LSRP. These elevations are well resolved in both the Meso Eta and MM5 models. Figures 2a and 2b show the narrow finger-like Central Mountain valleys, which are aligned in a northwest to southeast orientation in Zone 32. These valleys located in west to east order are the Big Lost River, Little Lost River, and Birch Creek Valleys, which drain into the USRP. The Central Mountain Valleys decrease in elevation from approximately 1.9 km at their northwest entrance point to roughly 1.6 km at their opening to the USRP and are resolved slightly better in the MM5 versus the Meso Eta model.

b. Wind flow pattern

The normal wind flow over the SRP is characterized by upslope winds during the daytime hours and downslope winds at night (Stewart et al. 2002). Figure 2c is a schematic of the conceptualized SPCZ flow pattern over eastern Idaho with qualitative arrows indicating the prevailing wind direction over the Central Mountain valleys, USRP, and LSRP near the time of boundary genesis. Under certain synoptic patterns associated with the passage of a surface cold front across eastern Idaho, the 700-mb flow (arrows) aligns to a northwest direction over the narrow Central Mountain valleys (Big Lost River, Little Lost River, and Birch Creek). The 850-mb flow (arrows) shifts to a southwest to west direction over the eastern Magic Valley and LSRP and to a north to northeast direction over the USRP. This forms a convergence zone (dashed line) initially over the USRP (from Mud Lake to north of Idaho Falls), and depending on the strength of the low-level winds over the USRP versus the LSRP, the boundary may move across the USRP; remain quasi-stationary; or propagate south into the LSRP.

c. Seasonal climatology and characteristics

The seasonal cycle of the SPCZ is categorized by maximum frequency in the late fall and winter seasons specifically from October through February when cold fronts are climatologically more common in eastern Idaho (Andretta 1999). Episodes of the SPCZ are less frequent during the spring and summer months especially from June through August. Tables 2a and 2b illustrate the dates of the 27 SPCZ cases, pattern types, and approximate times of the formation, persistence, and dissipation phases. The Type A pattern occurred in 78% of the cases and most of the SPCZ events occurred between 0700 UTC (0000 MST) and 2300 UTC (1600 MST).

TABLE 2a: Dates, Approximate Phase Times, and Z Coefficients of Type A SPCZs

Date	Type	Formation Phase (UTC)	Persistence Phase (UTC)	Dissipation Phase (UTC)	Z Coefficient
11/26/1995	A	13-16	17-20	21-23	0.87
12/05/1995	A	18-19	20-22	23-00 (6th)	0.86
01/17/1996	A	10-12	13-16	17-19	1.01
01/28/1996	A	08-09	10-13	14-15	0.44
04/13/1996	A	14-17	18-20	21-23	0.93
09/22/1996	A	11-13	14-17	18-20	0.75
10/16/1996	A	13-16	17-20	21-23	0.74
10/25/1996	A	13-16	17-20	21-23	0.58
10/11/1997	A	15-18	19-21	22-23	0.88
10/04/1998	A	21-22	23-00 (5th)	01-02 (5th)	1.35
11/09/1998	A	23 (8th)-01	02-03	04-06	0.84
11/18/1998	A	09-11	12-14	15-17	0.49
11/24/1998	A	00-01	02-04	05-06	0.49
01/27/1999	A	08-10	11-13	14-16	0.72
10/15/1999	A	21-22	23-01 (16th)	02-04	0.83
11/18/1999	A	14-15	16-17	18-19	1.24
12/13/1999	A	15-17	18-20	21-22	0.33
11/01/2000	A	14-16	17-21	22-23	0.76
11/28/2000	A	07-08	09-13	14-16	0.67
12/17/2000	A	13-14	15-17	18-20	0.35
10/11/2001	A	16-18	19-22	22-24	0.62

TABLE 2b: Dates, Approximate Phase Times, and Z Coefficients of Type B SPCZs

Date	Type	Formation Phase (UTC)	Persistence Phase (UTC)	Dissipation Phase (UTC)	Z Coefficient
01/05/1996	B	01-03	04-06	07-08	0.39
10/24/1997	B	04-08	09-13	14-17	1.47
01/20/1998	B	23 (19th)-01	02-04	05-07	0.52
12/25/2000	B	00-02	03-07	08-09	0.96
02/07/2001	B	02-03	04-07	08-10	1.90
11/27/2001	B	23 (26th)-00	01-04	04-06	1.16

The SPCZ produces bands of clouds and precipitation, usually in the form of light to moderate precipitation under the most synoptically favorable circumstances. During the colder months of the year, the SPCZ can generate several inches of snow in the SRP warranting operational meteorologists to issue weather advisories and storm warnings. A less-organized and weaker SPCZ, by comparison, may result only in clouds or a wind-shift boundary with little or no precipitation. The movement of the SPCZ is similar to a surface cold frontal passage with temperatures falling as the boundary passes a given point.

While not a primary ingredient for SPCZ formation, atmospheric stability may add to precipitation totals. Convective activity may develop in the SPCZ inducing bursts of moderate to heavy rain or snow (Andretta and Hazen 1998). For example, the SPCZ event of 11 October 2001 was characterized by a line of strong thunderstorms (40 to 50 dBZ) and lightning activity coincident with the leading edge of the convergence boundary. This convective activity is correlated with steep 850 to 500 mb lapse rates of -5.5 to -7 °C km^{-1} across the USRP and LSRP.

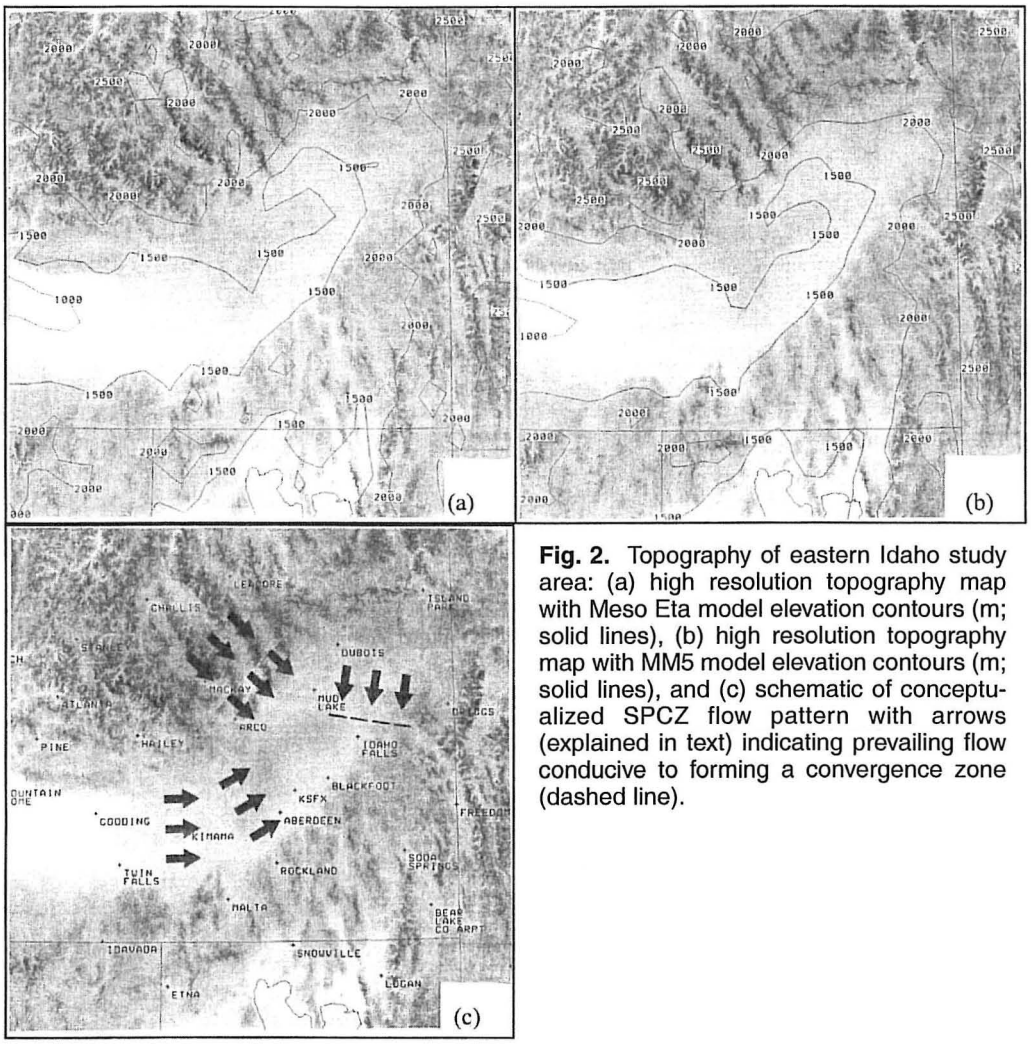

Fig. 2. Topography of eastern Idaho study area: (a) high resolution topography map with Meso Eta model elevation contours (m; solid lines), (b) high resolution topography map with MM5 model elevation contours (m; solid lines), and (c) schematic of conceptualized SPCZ flow pattern with arrows (explained in text) indicating prevailing flow conducive to forming a convergence zone (dashed line).

3. Synoptic Climatology (12 to 24 hours forecast time)

As indicated in Tables 2a and 2b, the synoptic flow conducive to SPCZ formation is grouped into two patterns (Type A and Type B), which in large measure are driven by the low and midlevel pressure gradients (Andretta and Hazen 1998). The Type A pattern was more common (78%) than the Type B pattern over the period of study (Tables 2a and 2b). The key synoptic indicators for both types are listed below.

a. Type A pattern

The Type A pattern is induced by the following antecedent synoptic conditions (Fig. 3a):

1) A broad to moderate amplitude 500-mb ridge with axis off coast of Washington and Oregon

2) A shallow, open, negatively or neutrally tilted 500-mb trough over western Idaho

3) A 500-mb jet (40 to 50 knots) oriented northwest to southeast over central Nevada and ejecting southwest to northeast over southern Utah

4) A 700-mb low over central or eastern Idaho with northwesterly flow (20 to 35 knots) over eastern Idaho

5) A 700-mb local vorticity maximum may be situated over the Upper or Lower Snake River Plain

6) A (usually closed) surface low located over central or eastern Wyoming with surface high pressure over eastern Oregon (mean sea-level pressure gradient of 4 to 7 mb from Burley to Rexburg, Idaho)

7) A surface Pacific cold front extending southwest from central or eastern Wyoming across central Utah or western Colorado

8) Boundary layer relative humidities of 85 to 100% over the Snake River Plain with low-level moisture maximum over eastern Idaho

b. Type B pattern

The Type B pattern is induced by the following antecedent synoptic conditions (Fig. 3b):

1) A moderate amplitude 500-mb ridge with axis off coast of Washington and Oregon

2) A (usually closed) 500-mb low (-25 to -35 °C) over northern Utah, northern Nevada or central Idaho (500-mb trough axis is usually neutrally or positively tilted)

3) A 500-mb jet (50 to 60 knots) oriented northwest to southeast over eastern Oregon or western Nevada and ejecting southwest to northeast across southern Utah or northern Arizona

4) A 700-mb low over southern Idaho or northern Utah with north to northwesterly flow (25 to 40 knots) over eastern Idaho

5) A 700-mb local vorticity maximum may be situated over the Lower Snake River Plain

6) A (usually closed) surface low located over northwest Colorado or northern Utah with surface high pres-

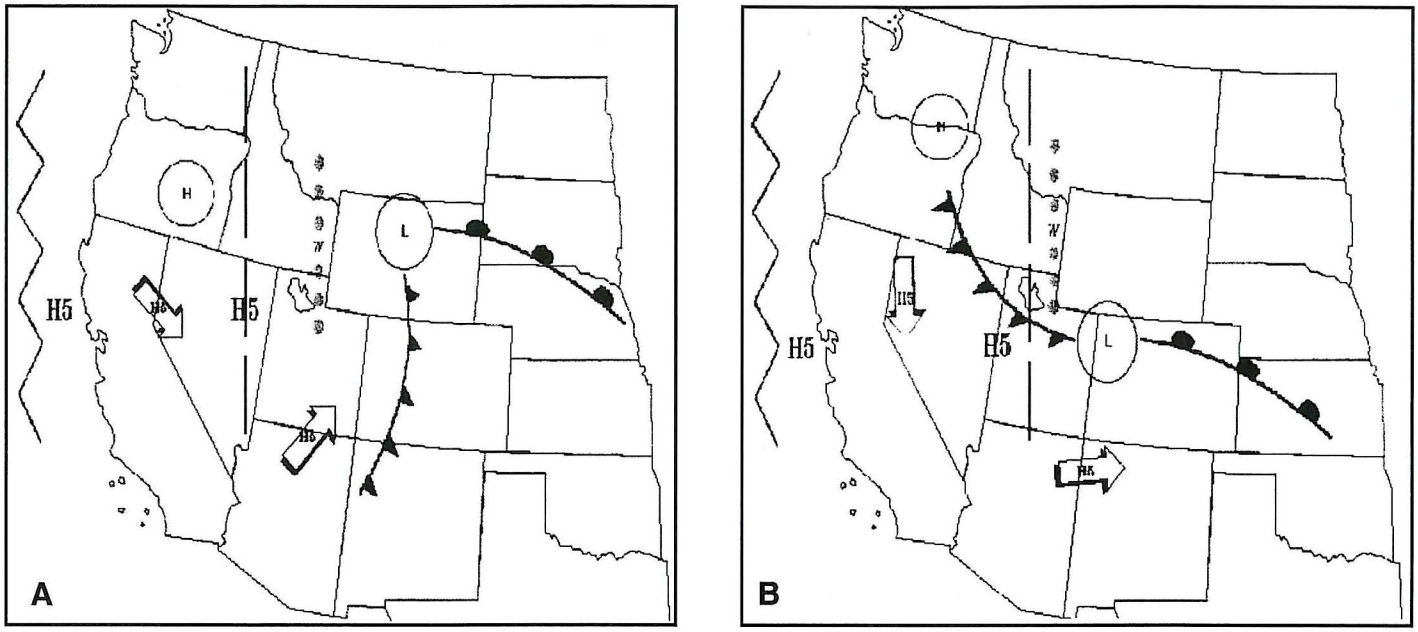

Fig. 3. Synoptic patterns: (a) Type A SPCZ synoptic pattern with standard weather symbol conventions and (b) Type B SPCZ synoptic pattern with standard weather symbol conventions.

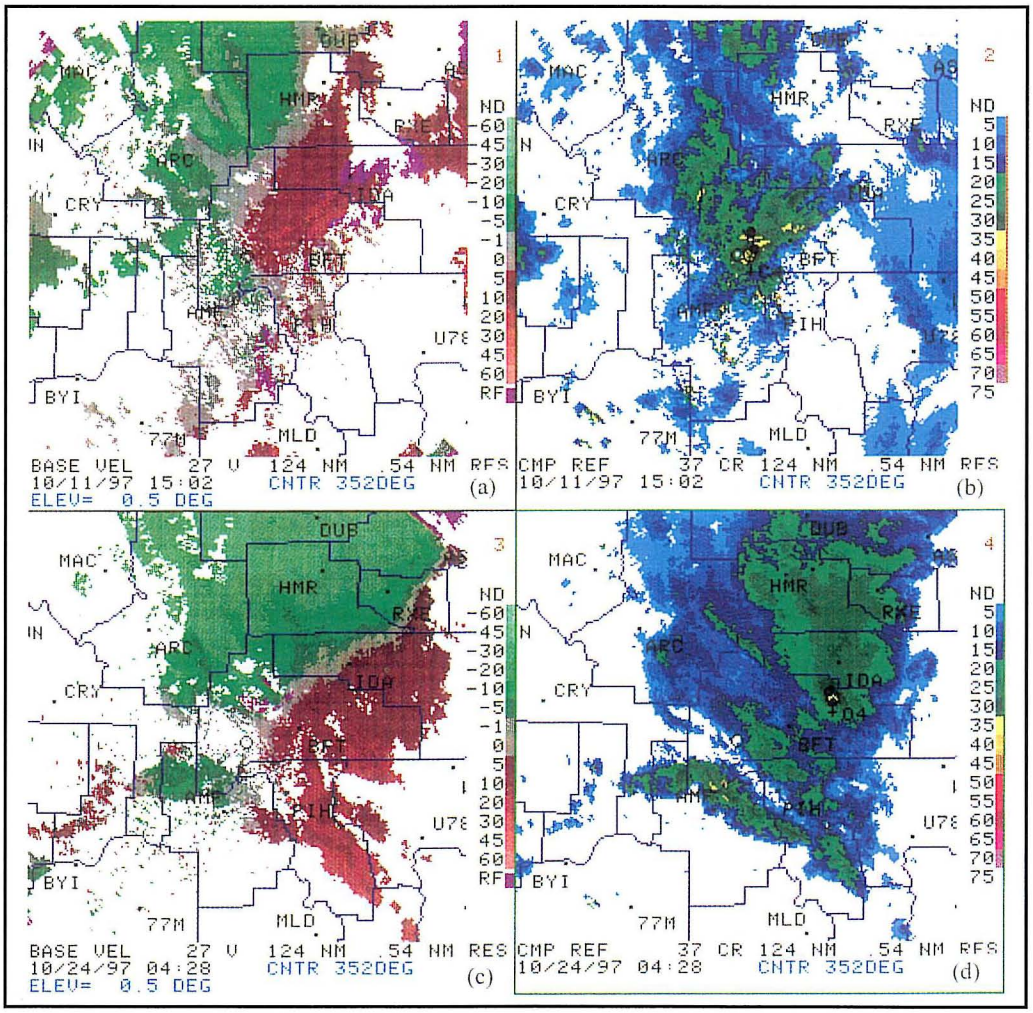

Fig. 4. Formation Stage for two cases - Type A: (a) WSR-88D (0.5 degree angle) Base Velocity (kt) at 1502 UTC 11 October 1997 and (b) WSR-88D Composite Reflectivity (dBZ) at 1502 UTC 11 October 1997; and Type B: (c) WSR-88D (0.5 degree angle) Base Velocity (kt) at 0428 UTC 24 October 1997 and (d) WSR-88D Composite Reflectivity (dBZ) at 0428 UTC 24 October 1997.

sure over eastern Washington (mean sea-level pressure gradient of 4 to 8 mb from Burley to Rexburg, Idaho)

7) A surface Pacific/Arctic cold front extending northwest from northern Utah to western Idaho

8) Boundary layer relative humidities of 85 to 100% over the Snake River Plain with low-level moisture maximum over eastern Idaho

There are some noteworthy similarities and differences between the Type A and B patterns. Both types are induced by a surface cold frontal passage with high relative humidities in the boundary layer over eastern Idaho. There is sometimes a local vorticity maximum in the USRP or LSRP at the top of the boundary layer in both instances. The 500-mb, 700-mb and 850-mb height fields are usually lower and the mean sea-level pressure pattern is sometimes deeper in the Type B pattern. Another key difference is in the orientation of the upper-level synoptic pattern. The Type A pattern is associated with southwest flow aloft; the Type B pattern is linked to north or northwest flow aloft.

The Type A pattern is generally associated with Pacific maritime air regimes while the Type B pattern is typically associated with modified polar or Arctic air masses.

4. Wind Climatology (0 to 12 hours forecast time)

If either the Type A or Type B synoptic patterns are present for the 12 to 24 hour forecast time period, the operational forecaster should examine the 22-km Meso Eta low-level wind distributions to ascertain the amplitude of the SPCZ event.

a. Wind direction

The 850-mb flow in the Meso Eta model over the eastern Magic Valley and LSRP should be aligned in a southwest to west direction and in a north to northeast direction over the USRP. The 700-mb model flow should be aligned in a northwest direction from the Central Mountain Valleys to the LSRP. In the USRP, the wind direction (e.g., Rexburg (RXE), Idaho Falls (IDA)) should be 350 to 040 degrees; in the LSRP the wind direction (e.g., Pocatello (PIH), Blackfoot (BFT)) should be 230 to 280 degrees. Please see Figs. 1c and 1d for ARL/FRD and NWS METAR sensor locations.

b. Wind speed

The operational meteorologist can compute the Z coefficient, a variable used to ascertain the ratio of the average wind speeds in the USRP, (W_{USRP}) versus the LSRP, (W_{LSRP}). This calculation should be performed using the Meso Eta model surface wind data over the hours covering the beginning of the forecast formation stage to the end of the forecast persistence stage of the SPCZ. This time interval corresponds with the development and maturity of the SPCZ, as explained below in the radar section of this manuscript. The equations used to compute W_{USRP}, W_{LSRP}, and the Z coefficient include:

$$W_{USRP} = [\sum_{1}^{9} \text{USRP wind speeds}] / 9 \quad (1)$$

$$W_{LSRP} = [\sum_{1}^{6} \text{LSRP wind speeds}] / 6 \quad (2)$$

$$Z = [\, W_{USRP} * W_{LSRP}^{-1} \,] \quad (3)$$

Figure 1c shows the locations of the ARL/FRD mesonet stations used in this manuscript. The nine stations (to the nearest Meso Eta grid point) used in the USRP wind computation include: Monteview (MON), Loft (LOF), Terreton (TER), Rover (ROV), Roberts (ROB), Hamer (HAM), EBR2 (EBR), Kettle Butte (KET), and Idaho Falls (IDA).

The six stations (to the nearest Meso Eta grid point) used in the LSRP wind computation include: Taber (TAB), Blackfoot (BLK), Aberdeen (ABD), Fort Hall (FOH) (near PIH), Richfield (RIC), and Minidoka (MIN).

The Z coefficient computations may be "fine-tuned" from model predictors by using the observed ARL/FRD 15-m wind distributions as the forecast SPCZ event approaches real-time development. Tables 2a and 2b show the Z coefficients for all 27 SPCZ cases based on the ARL/FRD mesonet wind climatology. For the case of ($0 < Z < 1$), the Z value would indicate that the southwest to west winds in the LSRP were stronger than the north to northeast winds in the USRP, resulting in a more eastward-moving SPCZ. This also implies a more sheared environment for the SPCZ with precipitation located generally from RXE to IDA in the USRP with lesser amounts in the LSRP. A case of ($Z \sim 1$) implies a more long-lived and nearly stationary SPCZ with more widespread precipitation across the entire SRP. Finally, the case of ($Z > 1$) suggests that the SPCZ progresses southward from the USRP (genesis region) to the LSRP (mature-dissipation region) with more widespread precipitation in the LSRP.

Based on these three Z classifications for the SPCZ cases in Tables 2a and 2b, equations were derived to explain the relationship between the mean Z coefficients and the average observed liquid water precipitation for IDA, (P_{IDA}) and PIH, (P_{PIH}). This assumed forcing by boundary layer convergence *alone* from the beginning of the formation stage (t hours) to the end of the persistence phase (t + dt hours). These SPCZ life cycle times were selected due to the correspondence with the beginning and ending times of precipitation for IDA and PIH, key stations situated in the path of the mesoscale boundary. Thus, given these parameterizations and temporal limits, the following relationships were computed for (P_{IDA}) and (P_{PIH}):

For the ($0 < Z < 1$) case:

$$P_{IDA} \sim 0.040 \int_{t}^{t+dt} Z\, dt \,;\, P_{PIH} \sim 0.072 \int_{t}^{t+dt} Z\, dt \quad (4)$$

For the ($Z \sim 1$) case:

$$P_{IDA} \sim 0.010 \int_{t}^{t+dt} Z\, dt \,;\, P_{PIH} \sim 0.056 \int_{t}^{t+dt} Z\, dt \quad (5)$$

For the ($Z > 1$) case:

$$P_{IDA} \sim 0.013 \int_{t}^{t+dt} Z\, dt \,;\, P_{PIH} \sim 0.031 \int_{t}^{t+dt} Z\, dt \quad (6)$$

As Tables 2a and 2b indicate, half of the Type B Patterns were correlated with ($Z > 1$); a majority of the Type A cases were linked to Z coefficients less than one but greater than zero.

5. WSR-88D Climatology (0 to 6 hours forecast time)

The SPCZ radar climatology for the Type A and Type B patterns is illustrated for two cases: 11 October 1997 (Type A) and 24 October 1997 (Type B). As noted by Andretta and Hazen (1998), the SPCZ can be divided into various stages based on radar and mesonet wind signatures. Accordingly, the NWS (KSFX) radar data are presented in both cases for the formation (Fig. 4), persistence (Fig. 5), and dissipation (Fig. 6) stages. The a and b panels (11 October 1997 - Case A) and c and d panels (24 October 1997 -

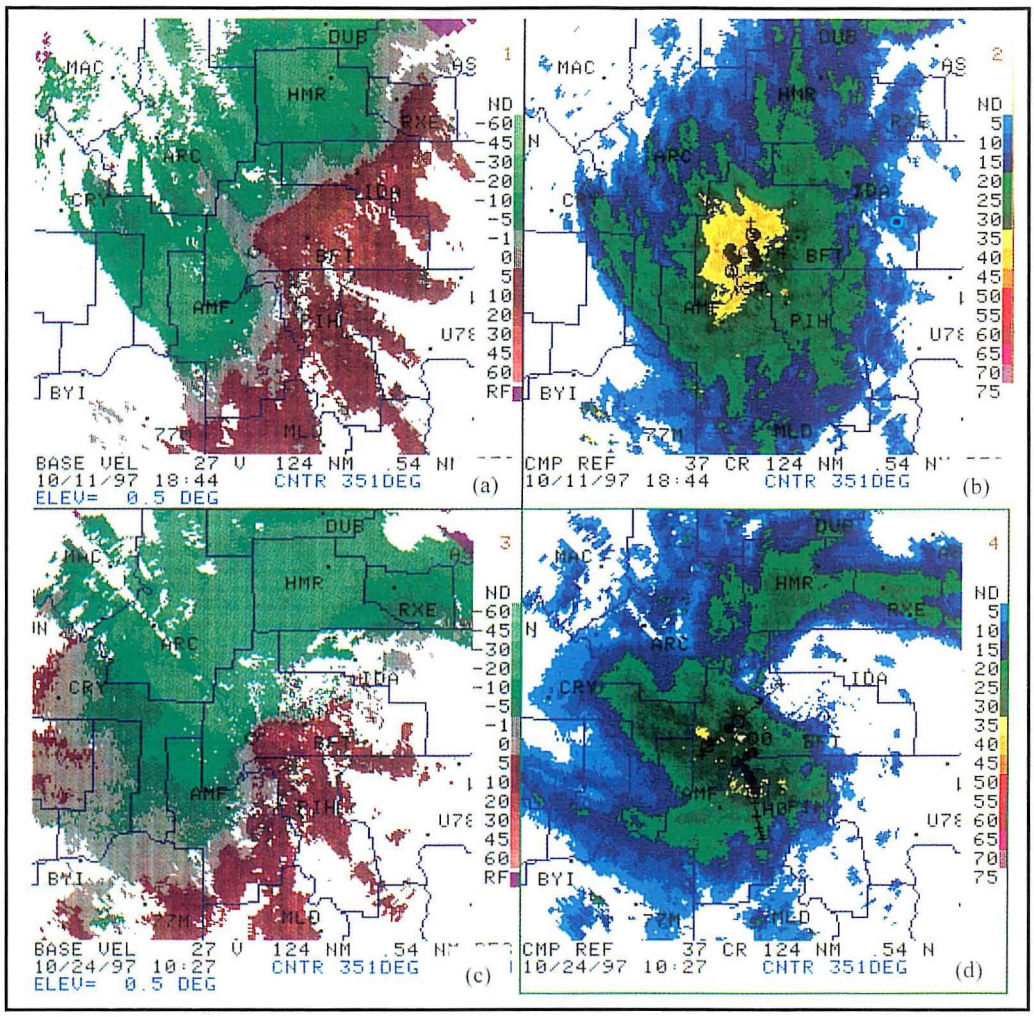

Fig. 5. Persistence Stage for two cases - Type A (data valid at 1844 UTC 11 October 1997): (a) WSR-88D (0.5 degree angle) Base Velocity (kt) and (b) WSR-88D Composite Reflectivity (dBZ); and Type B (data valid at 1027 UTC 24 October 1997): (c) WSR-88D (0.5 degree angle) Base Velocity (kt) and (d) WSR-88D Composite Reflectivity (dBZ).

Case B) are compared to highlight similarities and differences in the location and amplitude of two fields: the lowest tilt angle (0.5 degrees) of the base radial velocity and the composite reflectivity.

a. Formation stage

The formation stage typically lasts 1 to 2 hours in both the Type A and B patterns. Figures 4a and 4c indicate the development of the "Γ" shaped zero isodop with the region of zero base radial velocities stretching from Hamer (HMR) to American Falls (AMF) in Case A and from Rexburg (RXE) to Blackfoot (BFT) in Case B. This Γ shaped zero isodop is analogous to the classic "C" shaped signature associated with confluence on the WSR-88D (Brown and Wood 1987). The low-level winds at Idaho Falls (IDA) and RXE were north while at Aberdeen (ABD) and Pocatello (PIH) winds were in a southwest direction in both instances. In Case A, there was a separation (Fig. 4b) between the radar echoes associated with the developing SPCZ over the USRP and the weaker post-cold frontal reflectivity returns along the Idaho-Wyoming border. However, there was more of a merger between the post-frontal synoptic and mesoscale echoes in Case B (Fig. 4d) as the cold front sagged south of the Idaho-Utah border. The banding of the echoes was also more defined in Case B over the USRP notably parallel and downwind of the Central Mountain valleys. Despite these differences, radar echoes expanded in coverage over the SRP for the next few hours in both cases.

b. Persistence stage

The persistence stage generally lasts 2 to 4 hours in both patterns. This phase was marked by a nearly steady-state wind field with north to northeast winds over the USRP and southwest to west winds over the eastern Magic Valley and LSRP. Figs. 5a and 5c show the zero isodop oriented from RXE to BFT and extending from AMF to Malta (77M) in both cases. The Γ signature was clearly defined and composite reflectivities reached peak intensity over the USRP and LSRP during the mature stage (Andretta and Hazen 1998). In Case A, there was a large concave-shaped field of light to moderate (25 to 35 dBZ) reflectivity returns covering the SRP (Fig. 5b). Moderate to heavy snow (35 to 45 dBZ) associated with localized convective activity was observed west of BFT. Snow amounts of 1 to 4 inches were recorded by weather spotters from IDA to PIH. By comparison, the echo returns in Case B (Fig. 5d) were situated over the LSRP with IDA more removed from the echoes, possibly indicative of the drier air aloft and cold upper-level low pressure system migrating south along the Continental Divide. During this phase, the echoes were most persistent over the LSRP in Case B. This resulted in heavy snowfall, generally 5 to 8 inches, from BFT to PIH in the LSRP versus 1 to 3 inches from IDA to RXE in the USRP.

c. Dissipation stage

The dissipation phase of the SPCZ varies in length from 1 to 2 hours. The base velocity charts in Figs. 6a and

6c show the ambiguously defined zero isodop extending from RXE to BFT. The northwest to north flow over the USRP had intruded into the LSRP mixing out the low-level wind convergence field and signaling an end to the SPCZ (Andretta and Hazen 1998). In both cases, the wind shifted at PIH from southwest to northwest as the boundary moved south of the area, another indicator of SPCZ finality. As the Γ shaped isodop decayed, the composite reflectivity fields decreased in size and intensity in both cases with bands of light snow across the USRP and LSRP (Figs. 6b and 6d).

6. Multiple Regression Prediction Algorithm

The Z coefficients for the 27 SPCZ events were found to be correlated with different observed synoptic fields. After running various fields through a regression program on a test set of 17 cases and examining the statistical significance of them, a multiple regression equation was derived with these predictors (Wilks 1995):

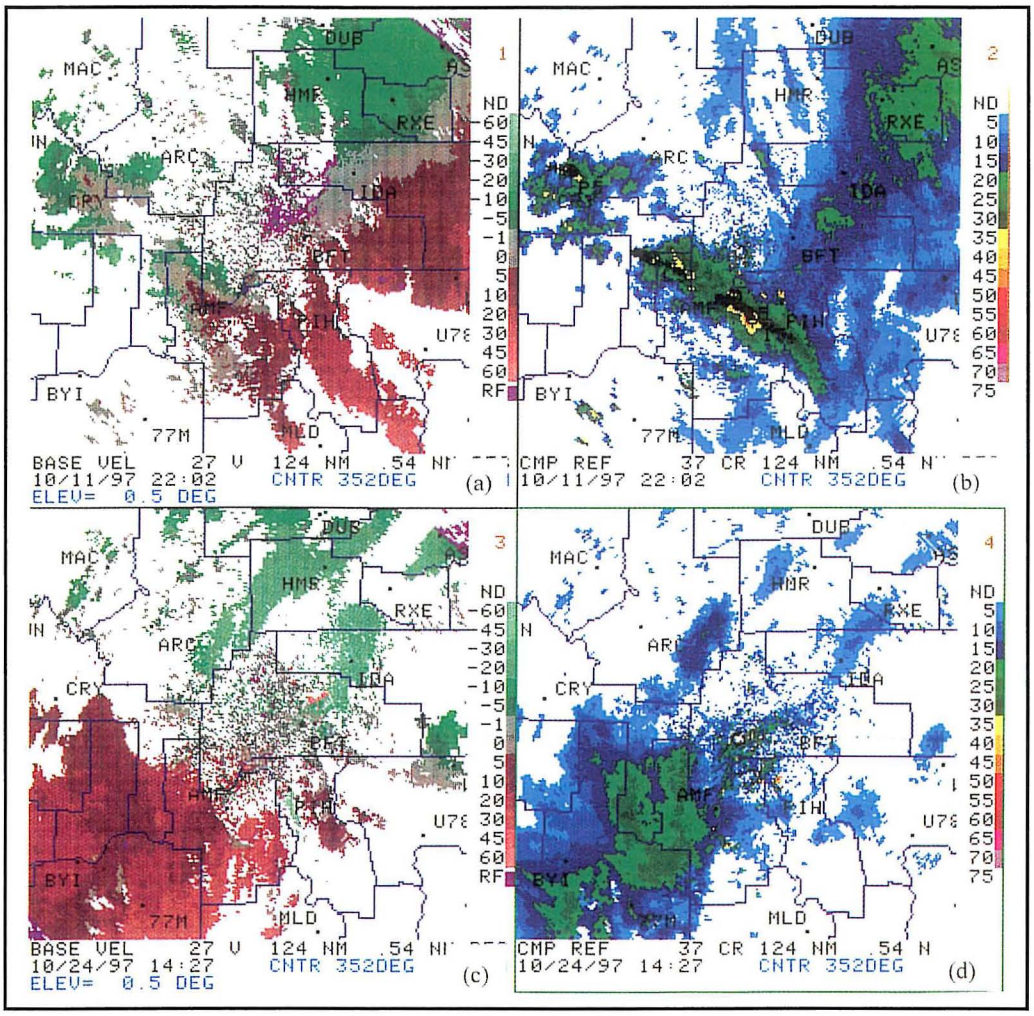

Fig. 6. Dissipation Stage for two cases - Type A (data valid at 2202 UTC 11 October 1997): (a) WSR-88D (0.5 degree angle) Base Velocity (kt) and (b) WSR-88D Composite Reflectivity (dBZ); and Type B (data valid at 1427 UTC 24 October 1997): (c) WSR-88D (0.5 degree angle) Base Velocity (kt) and (d) WSR-88D Composite Reflectivity (dBZ).

$$Z \sim 1.43 + 0.45 \sin(\theta_{IDA}) - 0.29 \sin(\theta_{PIH}) - 0.03\,[MSLP\,(Y - R)] - 0.01\,[H7\,(B - J)] \quad (7)$$

where:
Z = Z coefficient
θ_{IDA} = Surface wind direction at Idaho Falls (IDA), Idaho
θ_{PIH} = Surface wind direction at Pocatello (PIH), Idaho
MSLP (Y - R) = Mean sea-level pressure difference from Burley (BYI) to Rexburg (RXE), Idaho
H7 (B - J) = 700-mb height difference from Boise, Idaho to Jackson, Wyoming

Table 3 summarizes the Analysis of Variance (ANOVA) statistics generated from the multiple regression computations. The Pearson correlation coefficient for the variables was ~ 0.69. The 500-mb height difference from Boise, Idaho to Jackson, Wyoming was not statistically significant. As the mean sea-level pressure and 700-mb height differences become larger, the value of Z becomes smaller assuming a northerly surface wind at IDA and westerly surface wind at PIH. Equation (7) was vigorously tested using the 22-km Meso Eta model during several winter synoptic events

Table 3. Generic Analysis of Variance (ANOVA) Table

Source	df	SS	MS
Total	(n - 1) = 16	SST = 2.74883	
Regression	K = 4	SSR = 1.31874	MSR = 0.3296
Residual	(n - K - 1) = 12	SSE = 1.43009	MSE = 0.1191

in December 2001; the entire algorithm was encoded in a Tcl/Tk and Perl program designed by the author for easy accessibility by operational forecasters on local workstations. The numerical model guidance table for the SPCZ resembles other model guidance (e.g., FWC and MAV) tables and is produced from the 22-km Meso Eta model grids using a netCDF utility. The relevant data fields are displayed as a function of the model time steps. Accordingly, a sample program output for an SPCZ event, which occurred on 4 January 2002 is displayed in Fig 7. The noteworthy output variables include surface wind direction/speed at Idaho Falls and Pocatello, the Z coeffi-

Model: Meso Eta Month: 01 Day: 03 Year: 2002 Cycle: 1800Z
Model data was processed for the following variable(s) and level(s):

Variable	Units	Level
TEMP IDA	F	FHAG 2
TEMP PIH	F	FHAG 2
RH IDA	%	FHAG 2
RH PIH	%	FHAG 2
WDIR IDA	deg	FHAG 10
WDIR PIH	deg	FHAG 10
WSPD IDA	kt	FHAG 10
WSPD PIH	kt	FHAG 10
MSLP (Y-R)	mb	MSL
HT H7 (B-J)	m	MB 700
PROB SPCZ	%	
Z COEFFT		
PCPN IDA	in	SFC
PCPN PIH	in	SFC
SNOW IDA	in	SFC
SNOW PIH	in	SFC

Gradient: (Y-R) = Burley, ID to Rexburg, ID
(B-J) = Boise, ID to Jackson, WY

Meso Eta Guidance 01/03/2002 1800Z

Time	18	21	00	03	06	09	12	15	18	21	00
TEMP IDA	26	28	27	27	27	25	23	16	21	23	17
TEMP PIH	29	31	30	24	23	25	24	15	21	24	18
RH IDA	92	93	100	99	98	98	97	95	94	93	95
RH PIH	92	92	96	99	100	101	100	100	100	96	99
WDIR IDA	122	218	215	217	214	222	225	220	220	204	208
WDIR PIH	102	211	225	233	235	242	245	244	244	237	239
WSPD IDA	1	2	4	6	6	6	5	5	5	4	3
WSPD PIH	4	4	8	8	8	11	8	8	8	4	4
MSLP (Y-R)	1.8	3.5	1.9	2.2	2.0	0.0	2.2	1.6	1.1	0.4	-0.1
HT H7 (B-J)	12.0	40.4	20.2	29.9	27.9	41.7	33.7	28.2	33.9	28.7	26.3
PROB SPCZ	7.5	18.9	34.9	37.9	37.1	35.4	38.9	36.0	36.2	33.1	31.6
Z COEFFT	1.35	0.80	1.12	1.03	1.08	0.97	0.97	1.08	1.03	1.20	1.20
PCPN IDA	0.00	0.00	0.01	0.01	0.01	0.02	0.01	0.01	0.01	0.02	0.02
PCPN PIH	0.00	0.00	0.03	0.06	0.03	0.05	0.05	0.03	0.06	0.03	0.04
SNOW IDA	0.0	0.0	0.2	0.2	0.2	0.3	0.2	0.2	0.2	0.3	0.4
SNOW PIH	0.0	0.0	0.3	0.9	0.5	0.8	0.8	0.6	0.9	0.5	0.8

Code: 999 = Missing Data

Fig. 7. Multiple regression program output for 1800 UTC 3 January 2002.

cient (equation 7), probability of SPCZ occurrence, and estimates of precipitation (equations 4, 5, 6) and snowfall for IDA and PIH. The snowfall amounts for the two stations were computed using a conversion table based on ambient temperature and snow to liquid water equivalent ratio multipliers.

7. Case Study: 4 January 2002

This section explores the signatures and prediction methodologies discussed earlier. The 1800 UTC 3 January 2002 runs of the 22-km Meso Eta and 12-km MM5 models were utilized in this analysis.

a. Synoptic analysis

At 0000 UTC (1700 MST), the Meso Eta model indicated a 500-mb open trough of low pressure over eastern Oregon and western Idaho with a moderate amplitude ridge along the coast of Washington and Oregon or along 130W (Fig. 8a). An area of 50 to 60 knot winds was located on the west flank of the upper-level cyclone and moving across central Oregon and northern California. At the 700-mb level, an open trough of low pressure was located over central Colorado (Fig. 8b) with northwesterly flow of 10 to 20 knots over northern Nevada, northern Utah, and eastern Idaho. Figure 8c shows the mean sea-level pressure pattern in the MM5 model with a 1026-mb surface high over eastern Oregon and a 1019-mb surface low over eastern Idaho leading to the development of southwest winds in the eastern Magic Valley and the SRP. These forecast maps agreed closely with the Mesoscale Analysis and Prediction System Surface Assimilation System (MSAS) observed mean sea-level pattern and station data (Fig. 8d). The mean sea-level pressure difference was ~ 4 mb from Burley to Rexburg, Idaho. The surface cold front (not shown) was located over western Wyoming earlier in the afternoon of 4 January 2002. The MM5 boundary layer moisture charts (not shown) indicated 85 to 95% relative humidities over the SRP at 0000 UTC. These factors in the Meso Eta model collectively pointed to a Type B SPCZ event developing in the evening hours.

By 0600 UTC (2300 MST), the 500-mb pattern showed eastward progression with the upper-level low positioned over southern Idaho and along the Nevada-Utah border (Fig. 9a) with the upper jet axis over eastern Oregon and central Nevada. A 700-mb level, open wave was located in northern Arizona with northerly flow of 15 to 20 knots over central Idaho (Fig. 9b). The MM5 mean sea-level pressure and wind charts (Fig. 9c) showed a tighter gradient with an intrusion of northerly winds in the USRP. This result agreed with the surface observations (Fig. 9d). Both the MM5 and MSAS observations showed a 1021-mb surface low over the USRP with a mean sea-level pressure difference of ~ 3 mb from Burley to Rexburg, Idaho. The MM5 model accurately simulated the horizontal extent of the low-level moisture (not shown) over the SRP as the SPCZ developed.

b. WSR-88D and mesoscale analyses

The NWS (KSFX) WSR-88D base radial velocity (0.5 degrees) and composite reflectivity charts for 0300 UTC 4 January 2002 are illustrated in Figs.10a and 10b, respectively. An area of light snow developed from near Arco (ARC) to Idaho Falls (IDA) with the zero isodop extending from Rexburg (RXE) to near Arco. The KSFX VAD Wind Profile (Fig. 10c), used to show the vertical

structure of the SPCZ, illustrated southwest winds below 1.8 km (6000 feet) (all heights MSL) from 0200 to 0300 UTC. However, from 2.4 to 3.9 km (8000 to 13000 feet), the wind direction was chaotic from 0201 to 0231 UTC, becoming more unidirectional and westerly until 0300 UTC. The Local Analysis and Prediction System (LAPS) data in Fig. 10d indicated a 1021-mb surface low over the Central Mountains with ~ 3 mb difference in mean sea-level pressure from Burley (BYI) to Rexburg (RXE); surface winds were generally upslope over the SRP. The wind direction near Blue Dome (BLU) had shifted to a northwest direction. These factors suggested that an SPCZ was forming after 0300 UTC and continued until 0530 UTC.

By 0730 UTC, the area of snow had expanded from IDA to near American Falls (AMF) (Fig. 11b). The Γ signature was clearly defined with the zero isodop extending from IDA to the KSFX tower to AMF (Fig. 11a). Moderate to heavy snow was reported at both IDA and RXE coinciding with the location of the 30 to 35 dBZ echoes. The VAD Wind Profile (Fig. 11c) from 0632 to 0730 UTC indicated southwest winds of 15 to 20 knots below 2.1 km (7000 feet) with northwest winds from 2.1 to 4.2 km (7000 to 14000 feet). The actual convergence line was clearly indicated at 2.1 km (7000 feet) on the VWP; the surface observations in Fig. 11d delineated this convergence with north to northwest winds over the Central Mountain valleys and USRP merging with southwest winds in the LSRP. Surface temperatures across the USRP had fallen 3 to 5 °F as the boundary advanced southward into the LSRP. The persistence stage of the SPCZ lasted from about 0600 to 0800 UTC.

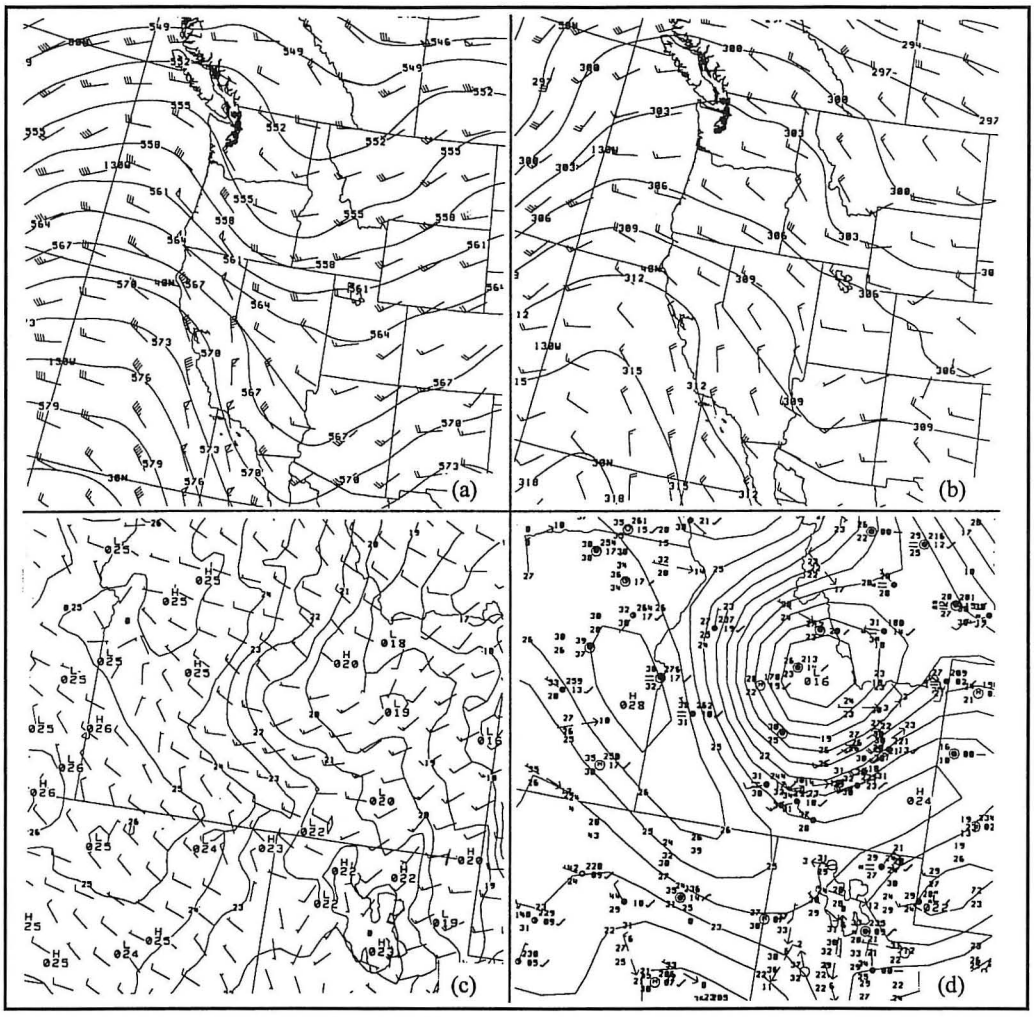

Fig. 8. Charts valid 0000 UTC (1700 MST) 4 January 2002: (a) Meso Eta 500-mb height contours (dm; solid lines) and wind barbs (each full barb 10 kt, flag 50 kt), (b) Meso Eta 700-mb height contours (dm; solid lines) and wind barbs (each full barb 10 kt, flag 50 kt), (c) MM5 mean sea-level pressure isobars (mb; solid lines) and surface winds (each full barb 10 kt, flag 50 kt) and (d) MSAS mean sea-level pressure analysis (mb; solid lines) with plotted data from ARL/FRD and NWS METAR station observations.

The dissipation phase was characterized by a diffuse zero isodop (Fig. 12a) and a weaker composite reflectivity field (Fig. 12b). The VAD Wind Profile (Fig. 12c) from 0859 to 0958 UTC displayed weaker southwest flow at 1.5 km (5000 feet), especially from 0923 to 0958 UTC. The northerly flow that developed from 2.4 to 4.2 km (8000 to 14000 feet) continued to mix out the low-level southwesterly flow below 2.1 km (7000 feet) and the SPCZ dissipated by 1100 UTC. The LAPS data (Fig. 12d) showed the mean sea-level pressure gradient had relaxed to 1 to 2 mb from Burley to Rexburg, further signaling the end of the SPCZ.

Figure 7 shows the Meso Eta model output from the regression program described in Section 6. As the table shows, the Z coefficient was between 0.97 and 1.08 over the SPCZ lifetime, suggesting a southward-moving SPCZ from the USRP to the LSRP. Probabilities of occurrence of 35 to 40% coincided with the SPCZ formation and persistence phases. Since the convergence was slightly elevated (2.1 km (7000 feet)) and above the ARL/FRD and NWS station elevations, the Meso Eta model did not initialize the observed surface northerly winds over the USRP satisfactorily. If this had not been the case, the forecast probabilities would have been even higher (~ 65%). The model precipitation estimates of 0.05 and 0.19 inches were obtained for Idaho Falls and Pocatello, respectively. These compared favorably with 0.05 and 0.09 inches, respectively, at the two stations. Snowfall estimates of 2 to 4 inches and 1 to 3 inches were recorded by weather spotters at Idaho Falls and Pocatello,

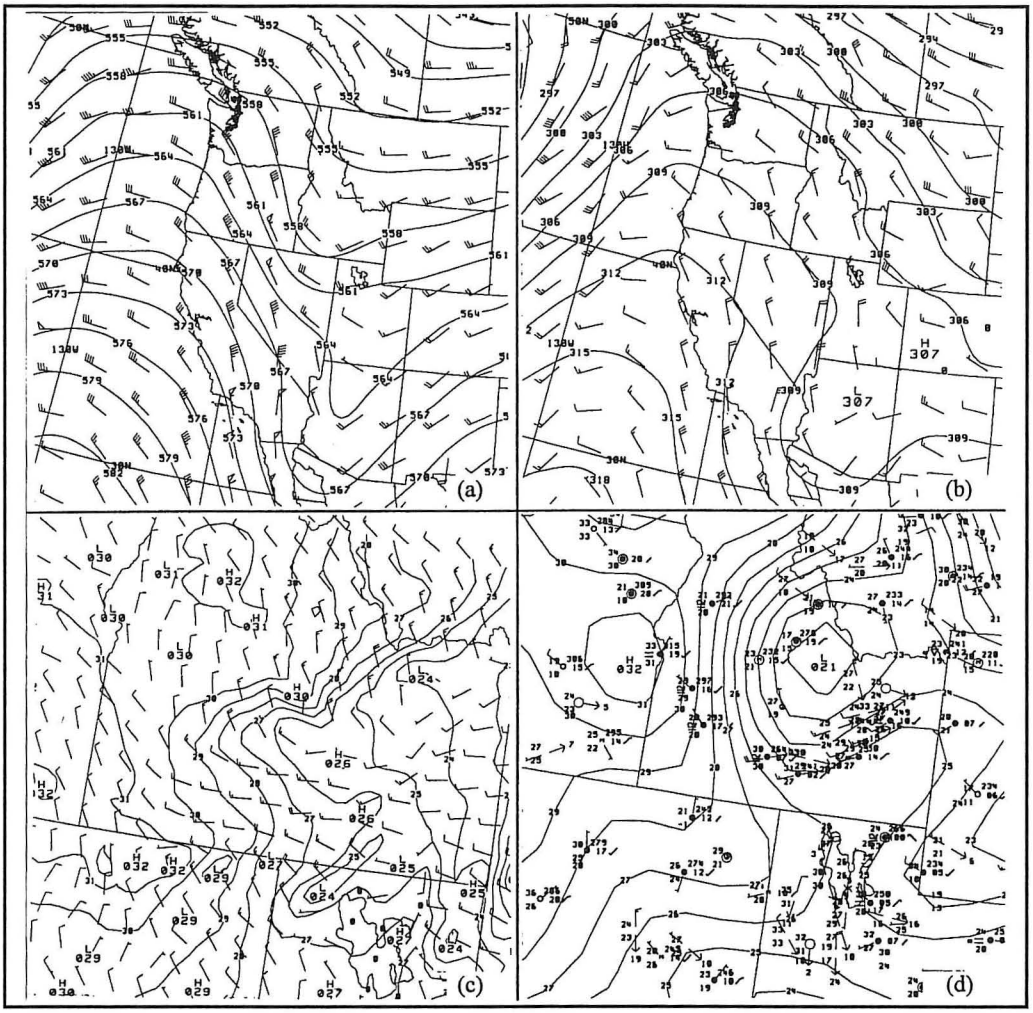

Fig. 9. As in Fig. 8, except charts valid 0600 UTC (2300 MST) 4 January 2002.

respectively. (At Rexburg, spotters recorded 6 to 8 inches of snow.) Figure 7 shows that from 0300 UTC to 1200 UTC, snowfall estimates of 0.9 and 3.0 inches were obtained for the two stations by the algorithm indicating general agreement between guidance and observations.

8. Future Considerations

The author hopes to run the multiple variable linear regression program (outlined in Section 6) on a faster LINUX PC using the 12-km MM5 model in order obtain more accurate output statistics. Other tasks include generating precipitation and snowfall estimates for other stations (e.g., Rexburg and Blackfoot) located in the path of the SPCZ and comparing these values with observations. Since the introduction of the SPCZ guidance table is new to forecasters, the author hopes to obtain considerable feedback for improving the presentation of the numerical output.

The existence of mesoscale vortices in some SPCZ events (Andretta and Hazen 1998) provides another challenging area of study. These features may be generated by local eddies inside the boundary and will require vertical cross-sectional analysis of the SPCZ vorticity and vertical velocity fields using higher resolution grids (e.g., 3 km) of the MM5 model. The origin of convective bands inside the SPCZ on reflectivity radar charts will require further investigation.

Finally, the impact of the SPCZ on local precipitation climatology will also need to be examined. Of interest, what is the exact percentage of SPCZ snowfall versus the total snowfall climatology for IDA and PIH? Do these amounts vary from year to year? These are questions that will need to be addressed in future studies.

9. Conclusions

A Snake River Plain Convergence Zone (SPCZ) is defined as the mesoscale boundary formed by the merger of low-level north to northeast winds in the Upper Snake River Plain with low-level southwest to west winds in the eastern Magic Valley and Lower Snake River Plain of eastern Idaho. This region of convergence is confined to the planetary boundary layer. The SPCZ is initiated by the passage of a surface cold front that aligns the flow to a northwest direction through the Big Lost, Little Lost, and Birch Creek Valleys in central Idaho. This manuscript examined a six-year climatology of this mesoscale feature based on mean antecedent synoptic characteristics obtained from 27 SPCZ cases covering the period from November 1995 to November 2001. The SPCZ was more common between October and March due to regional large-scale winter synoptic controls and cold frontal passages. The Type A pattern occurred in 78% of the cases; most of the SPCZ events occurred between 0700 UTC (0000 MST) and 2300 UTC (1600 MST).

The synoptic patterns conducive to SPCZ formation were grouped into Type A and Type B patterns with an examination of the noteworthy similarities and differences. Both types were induced by the passage of a surface cold front with high (85 to 100%) relative humidities in the boundary layer over eastern Idaho. A 700-mb local vorticity maximum in the USRP or LSRP is sometimes present in both instances. The 500-mb, 700-mb and 850-mb height and mean sea-level pressure fields were usually deeper in the Type B pattern. Another key difference was the orientation of the upper-level synoptic pattern. The Type A pattern was associated with southwest flow aloft; the Type B pattern was linked to north or northwest flow aloft. The Type A pattern was generally associated with Pacific maritime air regimes while the Type B

pattern was typically associated with modified polar or Arctic air masses.

The SPCZ wind climatology was explored using Meso Eta model data initially and then a blend of both model and NOAA/DOE ARL/FRD mesonet wind observations as the SPCZ reached real-time formation. An intensity scale (Z coefficient) was developed to identify the strength of the low-level wind flow in the USRP and the LSRP based on the wind observations. Depending on the ratio of the average valley wind speeds in the USRP versus the LSRP, precipitation may be more localized over the USRP ($0 < Z < 1$), widespread over the entire SRP ($Z \sim 1$), or more focused over the LSRP ($Z > 1$). Precipitation equations were derived from the Z classifications for both Idaho Falls and Pocatello, stations located in the path of the boundary.

The SPCZ radar signatures, derived from NWS (KSFX) WSR-88D base radial velocity (0.5 degrees) and composite reflectivity data, were presented with examples of the formation, persistence, and dissipation stages for two cases: 11 October 1997 (Type A pattern) and 24 October 1997 (Type B pattern). The formation stage was marked by development of the Γ shaped zero isodop stretching from roughly Rexburg (RXE) to Blackfoot (BFT) in the USRP. The SPCZ reached peak intensity during the persistence phase with a well-defined Γ shaped zero isodop and a large field of light to moderate precipitation over the SRP. The SPCZ ended as the north to northeast flow over the USRP intruded into the LSRP mixing out the low-level wind convergence field.

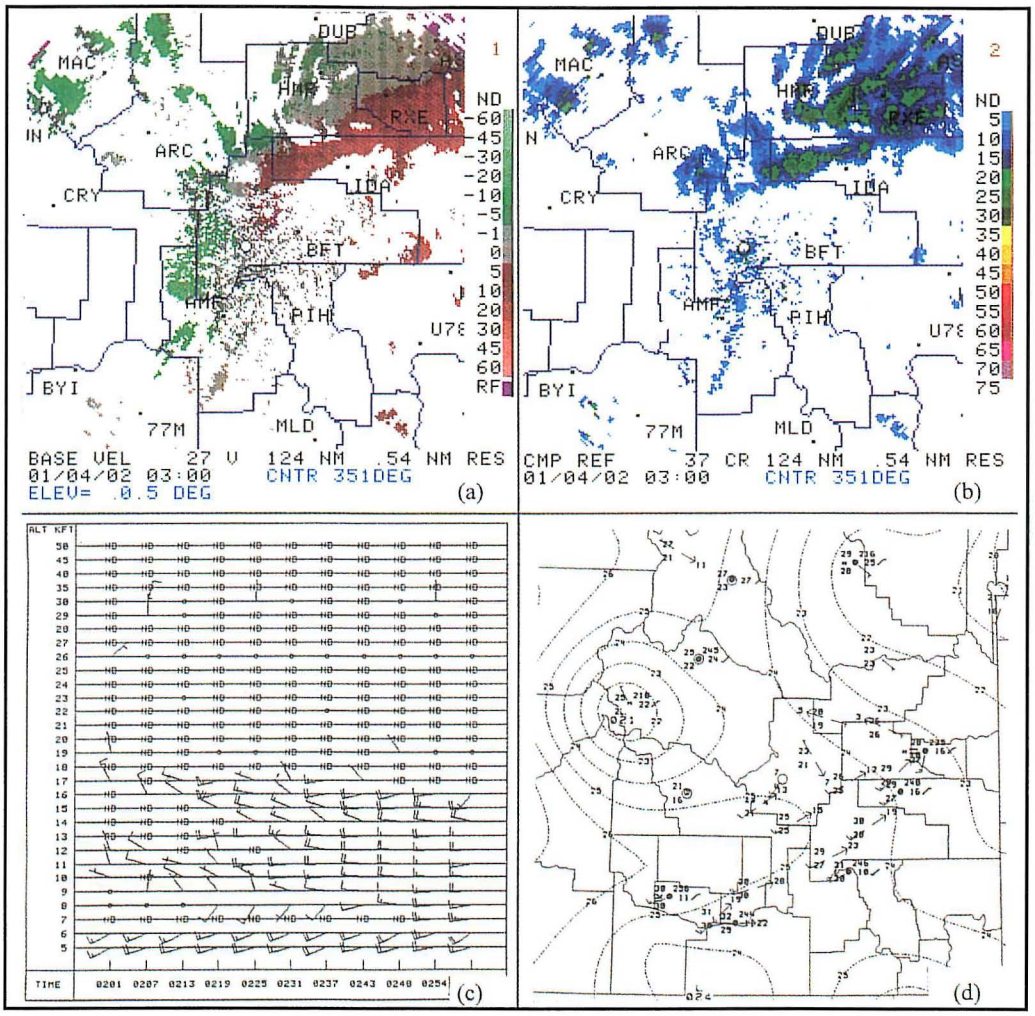

Fig. 10. Formation Stage: (a) WSR-88D (0.5 degree angle) Base Velocity (kt) and (b) WSR-88D Composite Reflectivity (dBZ) at 0300 UTC 4 January 2002, (c) WSR-88D VAD Wind Profile (kt) wind barbs (each full barb 10 kt, flag 50 kt) from 0201 to 0300 UTC 4 January 2002, and (d) LAPS mean sea-level pressure analysis (mb; dotted lines) with plotted data from ARL/FRD and NWS METAR station observations at 0300 UTC 4 January 2002.

A multiple regression equation was derived using several parameters for 17 SPCZ cases and encoded in a computer program for access by operational meteorologists on local workstations. This equation was tested on several SPCZ events in December 2001 using the 22-km Meso Eta model data fields. The output data was presented in a time-dependent guidance table with emphasis on the Z coefficient, probability of occurrence, and estimates of precipitation and snow amounts for Idaho Falls and Pocatello.

The multiple regression prediction scheme was applied to the SPCZ episode on 4 January 2002. This event matched the Type B SPCZ synoptic pattern. The regression output indicated a Z coefficient near 1.0 and a 35 to 40% probability of occurrence. There was general agreement between forecast and observed precipitation and snowfall amounts for Idaho Falls and Pocatello.

Acknowledgments

The author would like to thank the Science and Operations Officer (SOO) Dean Hazen, and forecasters: Rick Winther, Bill Wojcik, and Jack Messick from the NWS Forecast Office, Pocatello-Idaho Falls, Idaho for providing input on this study. Dr. Clifford Mass, Dr. Michael Meyers, and Paul Frisbie provided timely and constructive reviews of the manuscript.

Author

Thomas Andretta received his Bachelor of Science (1988) and Master of Science (1991) degrees in Atmospheric Science at the State University of New York (SUNY) at Stony Brook. He joined the National Weather

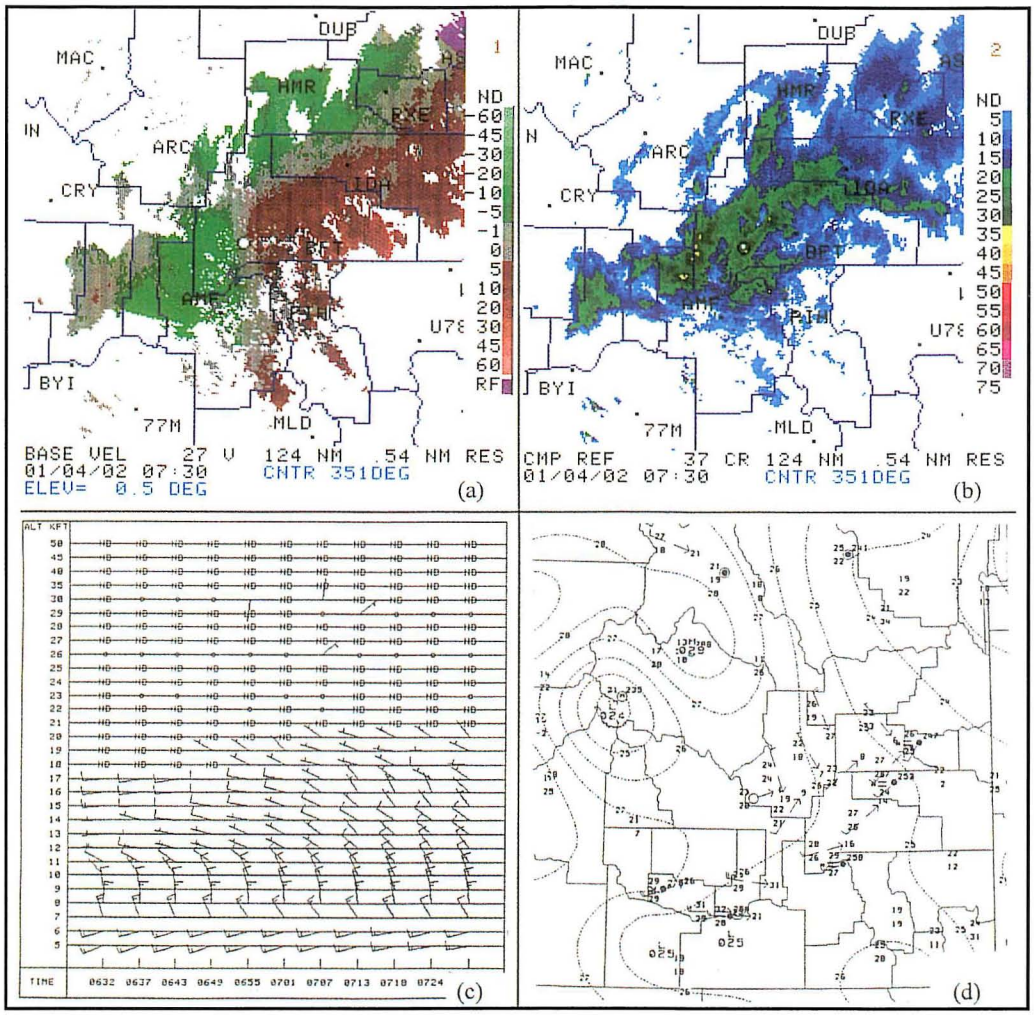

Fig. 11. Persistence Stage: (a) WSR-88D (0.5 degree angle) Base Velocity (kt) and (b) WSR-88D Composite Reflectivity (dBZ) at 0730 UTC 4 January 2002, (c) WSR-88D VAD Wind Profile (kt) wind barbs (each full barb 10 kt, flag 50 kt) from 0632 to 0730 UTC 4 January 2002, and (d) LAPS mean sea-level pressure analysis (mb; dotted lines) with plotted data from ARL/FRD and NWS METAR station observations at 0700 UTC 4 January 2002.

Service in May 1993 as a meteorologist intern at the Lake Charles, Louisiana office. He accepted a journeyman forecaster position in February 1995 and a lead forecaster position in February 1998 at the National Weather Service office in Pocatello, Idaho. His interests include boundary layer meteorology in complex terrain, fog physics, precipitation climatology, tornado climatology, and designing meteorological computer applications on multiple platforms.

References

Andretta, T. A., 1999: Harmonic analysis of precipitation data in eastern Idaho. *Natl. Wea. Digest*, 23:1-2, 31-40.

_____, and D. S. Hazen, 1998: Doppler radar analysis of a Snake River Plain convergence event. *Wea. Forecasting*, 13, 482-491.

Brown, R.A., and V.T. Wood, 1987: A guide for interpreting Doppler velocity patterns. *NEXRAD Joint System Program Office Report R400-DV-101.*, pp 51. [Available from the National Weather Service Office, 1945 Beechcraft Ave, Pocatello, Idaho, 83204.]

Chien, Fang-Ching, and C.F. Mass, 1997: Interaction of a warm-season frontal system with the coastal mountains of the western United States, Part II: Evolution of a Puget Sound convergence zone. *Mon. Wea. Rev.*, 125, 1730-1752.

Dudhia, J., D. Gill, Y-R. Guo, D. Hansen, K. Manning and W. Wang, 1999: PSU/NCAR Mesoscale Modeling System Tutorial Class Notes and Users' Guide: MM5 Modeling System Version 2. Mesoscale and Microscale Meteorology Division, NCAR, 182 pp.

Grell, G., J. Dudhia and D. Stauffer, 1995: A Description of the Fifth Generation Penn State/NCAR Mesoscale Model (MM5). Mesoscale and Microscale Meteorology Division, NCAR/TN-398+STR, 117pp.

Manikin, G., M. Baldwin, W. Collins, J. Gerrity, D. Keyser, Y. Lin, K. Mitchell and E. Rogers, 2000: Changes to the NCEP Meso Eta runs: Extended range, added input, added output, convective changes. *NWS Technical Procedures Bulletin*, 465, NOAA/NWS.

Mass, C.F., 1981: Topographically forced convergence in western Washington State. *Mon. Wea. Rev.*, 109, 1335-1347.

_____, and D.P. Dempsey, 1985: A topographically-forced convergence line in the lee of the Olympic Mountains. *Mon. Wea. Rev.*, 113, 659-663.

Rasmussen, R.M., and Coauthors, 1992: Winter Icing and Storms Project (WISP). *Bull. Amer. Meteor. Soc.*, 73, 951-976.

Staudenmaier, Jr., M., 1996: A description of the Meso Eta model. *Western Region Technical Attachment*, 96-06.

Stewart, J.Q., C.D. Whiteman, W.J. Steenburgh and X. Bian, 2002: A climatological study of thermally driven wind systems of the U.S. Intermountain West. *Bull. Amer. Meteor. Soc.*, 83, 699-708.

Szoke, E. J., and J. L. Wiesmueller, 1989: Mesoscale structure of winter snowstorms in northeast Colorado as revealed by Doppler radar: Potential for short range forecasting. Preprints, *12th Conf. on Weather and Forecasting*, Monterey, CA, Amer. Meteor. Soc., 384-389.

Wesley, D. A., R. M. Rasmussen and B. C. Bernstein, 1995: Snowfall associated with a terrain-generated convergence zone during the Winter Icing and Storms Project. *Mon. Wea. Rev.*, 123, 2957-2977.

Whitney, M. W., R. L. Doherty and B. R. Colman, 1993: A methodology for predicting the Puget Sound convergence zone and its associated weather. *Wea. Forecasting*, 8, 214-222.

Wilks, D. S., 1995: *Statistical methods in atmospheric sciences*. Academic Press, San Diego, ISDN 0-12-751965-3, 464 pp.

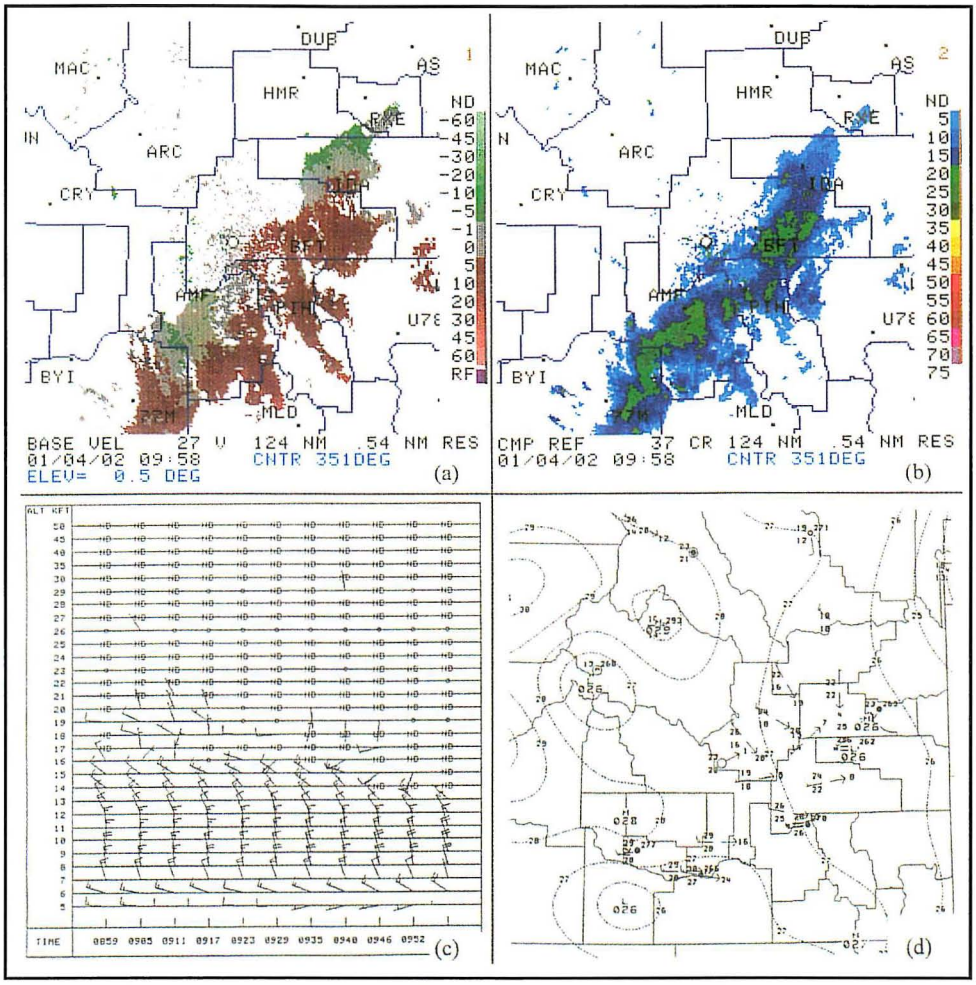

Fig. 12. Dissipation Stage: (a) WSR-88D (0.5 degree angle) Base Velocity (kt) and (b) WSR-88D Composite Reflectivity (dBZ) at 0958 UTC 4 January 2002, (c) WSR-88D VAD Wind Profile (kt) wind barbs (each full barb 10 kt, flag 50 kt) from 0859 to 0958 UTC 4 January 2002 and (d) LAPS mean sea-level pressure analysis (mb; dotted lines) with plotted data from ARL/FRD and NWS METAR station observations at 1000 UTC 4 January 2002.